

An Versatile Distinction Structure Based Haze Elimination Method

¹Y.Bindu, ²R.Venkateswarlu

¹PG Scholar, Dept. of ECE, Narayana Engineering College, Nellore, AP, India.

² Associate Professor, Dept. of ECE, Narayana Engineering College, Nellore, AP, India.

Abstract: Fog cover is by and large present in open air scenes, which restricts the potential for effective data extraction from pictures. In this paper, the objective of the created algorithm is to acquire an optimal transmission delineate well as to expel fogs from a solitary information picture. To take care of the issue, we meticulously dissect the optical model and recast the underlying transmission delineates an extra limit earlier. For better conservation of the outcomes, the distinction structure-safeguarding word reference could be realized with the end goal that the nearby consistency highlights of the transmission guide could be very much saved after coefficient shrinkage. Trial comes about demonstrate that the technique protects the natural appearance of the picture.

Index terms—visibility restoration, contrast restoration, single image dehazing, difference-structure-preservation, local depth consistency.

I. INTRODUCTION

Open air images are normally influenced by the nearness of mists or haze, which hinder image basic highlights, for example, edges. The perceivability, difference, and clarity of the scene are drastically debased^[1-2], which makes it hard to recognize objects thus it is important to recoup the first scene to enhance human recognizable proof capacity. Dehazing is an extraordinary instance of image restoration. Following Koschmiedar's law, a dim image is typically displayed by

$$I^c(x) = J^c(x)t(x) + A^c(1 - t(x)) \dots (1)$$

Note that our goal is to recover the underlying scene radiance, where $c \in (r, g, b)$, $I^c(x) \in R^c$ is the observed intensity at pixel x , $J^c(x)$ is the scene radiance or haze-free image^[3-5], A^c is the sky brightness for the whole image, and $t(x)$ is the scene transmission, which is correlated with the scene depth. Because A^c is usually determined empirically, the major difficulty of image dehazing is

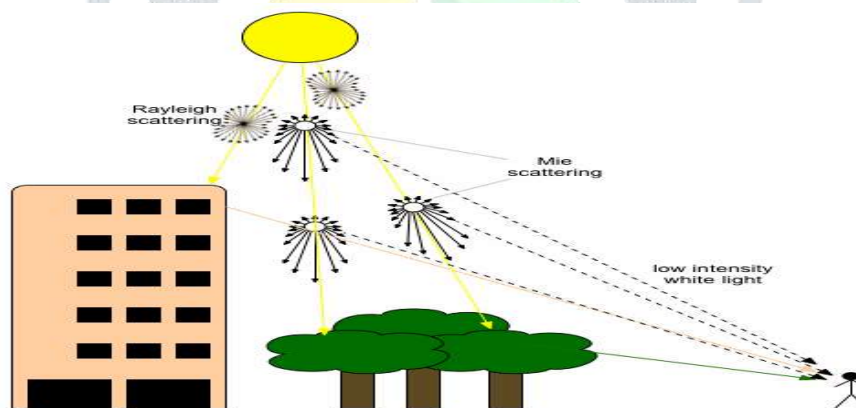


Fig1: Effects of atmospheric scattering

to compute $t(x)$. To make the not well postured issue tractable, numerous techniques utilize appropriate priors or extra data to appraise the transmission guide and after that get the without haze image.

II. DISTINCTION STRUCTURE- CONSERVATION PRECEDING

Following the dialog above, deciding how to explore the regularization that can precisely mirror the nearby consistency turns into a basic point in our answer. To start with, we give a technique to gauge the neighborhood profundity consistency. What's more, to utilize the locally reliable profundity as a regularize, we accept that a nearby fix can be approximated by a scanty direct mix of components from a neighbor premise set. All the more imperatively, through building the distinction structure - safeguarding word reference, the outcomes have exhibited that our approach is powerful at reestablishing images.

To this end, we recast the issue as finding an answer for transmission under scene limitations in the attainable range. Through the choice of parameters, an optimal transmission can be proposed and the total count process is compressed.

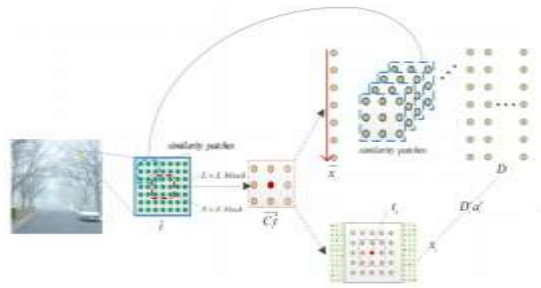


Fig2: The process of generating the training samples & Illustration of overlap

2.1 Spatially persistent extent

As in past writing, the depth edge consistency is chosen utilizing neighboring pixels. Thus, regardless of whether pixels lie on a similar depth is chosen just by the areas of the pixels. What's more, given C_i a chance to be the framework of ones, and we expect where s is the quantity of pixels in the image. The vector contains every one of the parts inside the $N \times N$ window. At that point, utilize a preparation piece to discover the preparation tests, as appeared in Fig 2. The least difficult and most productive path is to supplant $C_i \hat{t}$ with the encompassing preparing tests in the preparation square^[6-10]. We indicate as the segment test vector containing the pixels in the red $N \times N$ piece and mean x_j , where as the example vectors relating to the neighboring squares appeared in blue in Fig 2. Hence, we embrace the cosine similitude strategy to revise for the above mix-up. It can be effectively computed that

$$\text{sim}(x_i, y_j) = \cos\theta = \frac{x_i \cdot y_j}{\|x_i\| \cdot \|y_j\|} \dots (2)$$

We select it as a comparative example vector following the rule of BM3D, which suggests that comparative patches have comparative meager portrayals, let a_i be dictionary atoms speaking to Neighbor as opposed to averaging them with the closeness measure as the weights

$$(D_i, a_i) = \text{argmin} \|C_i \hat{t} - D_i a_i\|^2 + \lambda \|a_i\|_0 \dots (3)$$

$$= \text{argmin} \|X_i - D_i a_i\|^2 + \lambda \|a_i\|_0$$

Where X_i signifies the i th fix of size $N \times N$, and is the vector of codes as for dictionary D_i once the dictionary D_i and codes I have been adapted, each pixel of the transmission outline is assessed, so its esteem can be registered by averaging

$$t_k = \frac{1}{N^2} \sum_{i|k \in w_i} D_i^k a_i^k \dots (4)$$

Where k is a pixel in the transmission map, D_i and a_i represents the corresponding dictionary and its coefficients for each patch overlap, respectively.

2.2 Distinction -Structure- Conservation

Dictionary Obviously, D is a vital pointer, which can be viewed as the dictionary. Be that as it may, in view of hypothetical examination and exploratory perception, most word references depending on the All the more imperatively, spatial geometric structure can be pulverized among adjacent information by global Euclidean structure with the goal that the neighborhood consistency^[11-12] might be debilitated in Fig 3. In this paper, a novel technique called contrast structure-safeguarding is proposed, and it utilizes the comparable structures as completely as would be prudent and keeps up the contrasts between comparative fixes however much as could reasonably be expected. In light of the dialog over, the accompanying focuses ought to be considered:

- 1) From a measurable perspective, if the two examples are close or comparative, i.e., the separation between them is little or the comparability is high, they give little data; despite what might be expected, the distinction data ought to be extraordinary.
- 2) On the commence of likeness, to the extent it is conceivable to mirror the diverse condition of comparative examples, these examples give numerous data models. Likewise, since they are extremely scanty, the diverse examples can reflect more contrasts of data, and factual traits can likewise be assessed through these examples.
- 3) We can acquire patches from L closest neighbors^[13-15] to quantify the distinction data through Euclidean separation, while patches situated outside of the area can be overlooked. As indicated by these suspicions and to keep up the distinctions of the first information and express the neighborhood spatial connections, the components of the coefficient grid b_{ij} could quantify the particular data passed on by $I \times x$ and $j \times x$. For simplicity of portrayal, it is characterized as

$$\max \sum_{ij} (a_i - a_j)^2 b_{ij} \dots (5)$$

Where a_i and a_j are the weights of the original similarity patches x_i and x_j on the specific dictionary, and b_{ij} is the divergence between the patches in high-dimensional space.

$$b_{ij} = \begin{cases} \exp\left(-\frac{\tau}{\|x_i - x_j\|^2}\right), & x_j \in x_i \\ 0 & \text{others} \end{cases} \dots (6)$$

Here x_i signifies comparable neighborhood fixes around x_i , $\tau = 0.01$. For example, the symmetric weights b_{ij} force an overwhelming punishment if two comparative patches are far separated in the first image space however are mapped near each other. All things considered^[16], the capacity is expanded to ensure the assorted variety when the information are spoken to by the relating dictionary. At the end of the day, the progression looks to discover the lower-dimensional conservative subspace that proficiently saves the assorted variety among close-by information focuses. So also, we take note of the capacity that can hold the concealed related data:

$$\min \sum_i (a_i - \sum_j W_{ij} a_j)^2 \dots (7)$$

Where W_{ij} is a proclivity to quantify the similitude between the diverse patches. Complying with the above suppositions, we characterize a limitation: every datum fix X_i is associated just with its neighbors, so $W_{ij} = 0$ if X_j does not have a place with the arrangement of neighbors of x_i .

$$D = \operatorname{argmax} \frac{\sum_{ij} (a_i - a_j)^2 b_{ij}}{\sum_i (a_i - \sum_j W_{ij} a_j)^2} \dots (8)$$

$$J(D) = \max \frac{\sum_{ij} (a_i - a_j)^2 b_{ij}}{\sum_i (a_i - \sum_j W_{ij} a_j)^2}$$

$$= \frac{\sum_{ij} (D_i^T x_i - D_i^T x_j)^2 b_{ij}}{\sum_i D_i^T x_i (E - \sum_j W_{ij})^T (E - \sum_j W_{ij}) \sum_i x_i^T D_i}$$

$$= \frac{2D^T (\sum_i X_i h_{ii} X_i^T - \sum_{ij} X_i b_{ij} X_j^T) D}{D^T \sum_i x_i (E - W) (E - W)^T \sum_i x_i^T D}$$

$$= \frac{2D^T (X H X^T - X B X^T) D}{D^T X M X^T D}$$

$$= \frac{2D^T X L_h X^T D}{D^T X M X^T D} \dots (9)$$

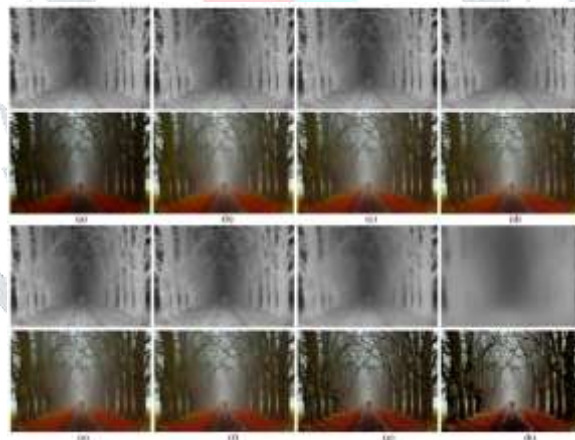


Fig3: The effect of the parameters

Where E is m order identity matrix and X is all the blocks with the pixel i as the center. Note that $L_h = H - B$ is called the difference-structure-preservation matrix, D_{ii} is a diagonal matrix equation(10) and is called the Laplacian similarity matrix. Using the Lagrange multiplier for the solution, we have

$$h_{ii} = \sum_j b_{ij}, M = (E - W)(E - W)^T \dots (10)$$

$$X L_h X^T D = \delta X M X^T D \dots (11)$$

Then, using the Cholesky decomposition for we obtain $X M X = G G^T$, where G is a lower triangular matrix. $Z = G^T D$, which we $1 = (G^{-1})^T Z$ substitute into the denominator where $S = G^{-1} X L_h X^T (G^{-1})^T$ is the symmetric matrix. In this way, we can easily obtain the solution.

2.3 The progression for DSPV display:

The fact that semantically meaningful image constructs are formed by spatially coherent contiguous patches suggests that the image is piecewise stationary^[17]. We propose a difference-structure-preservation variation model.

$$\begin{aligned} \inf_{t \in R} E_t &= \operatorname{argmin}_{\mu} \|\hat{t} - t\|^2 + \sum_i \|C_i \hat{t} - D_i a_i\|^2 + \sum_i \lambda \|a_i\|_0 \\ &= \operatorname{argmin}_{\mu} \|\hat{t} - t\|^2 + \left\| \hat{t} - \frac{1}{N^2} \sum_{i|k \in w_i} D_i^k a_i^k \right\| \dots (12) \end{aligned}$$

The main term of powers the closeness between the haze perception and the genuine scene image, and the parameter λ indicates the required level of nearness, as delineated in Fig. 4. We can see that the devotion term work is near the first esteem is huge. In that capacity, the impact of the control isn't huge and reestablished image changes are littler than those of the hazed image when the cycle step is consistent. This is likewise seen in our explore different avenues regarding images. It. The second term incorporates neighborhood comparability priors to shape a regularizing power. Obviously, the proposed approach is firmly identified with K-LLD, K-SVD, and BM3D. Be that as it may, it can be viewed as their expansion under the structure of the nearby depth consistency supposition. In addition, we pick an esteem that isn't to control meager codes. Contrasted and the previously mentioned algorithms, the most noteworthy distinction is the meaning of a distinction structure-conservation dictionary, which is a versatile similitude^[18] information network for demonstrating nearby portrayal. In another angle, it is additionally more predictable with the laws of material science, which recommends that the pixels have indistinguishable depth and will be debased to a similar degree. As we said in Section III, there are four stages to acquire the without haze image, which are depicted in Fig 5. To begin with, the issue can be isolated into the transmission outline environmental light issue. Like He's algorithm^[12], we have embraced two stages to estimate the genuine transmission delineate. In stage 2, we recast the underlying transmission delineate an extra boundary prior.

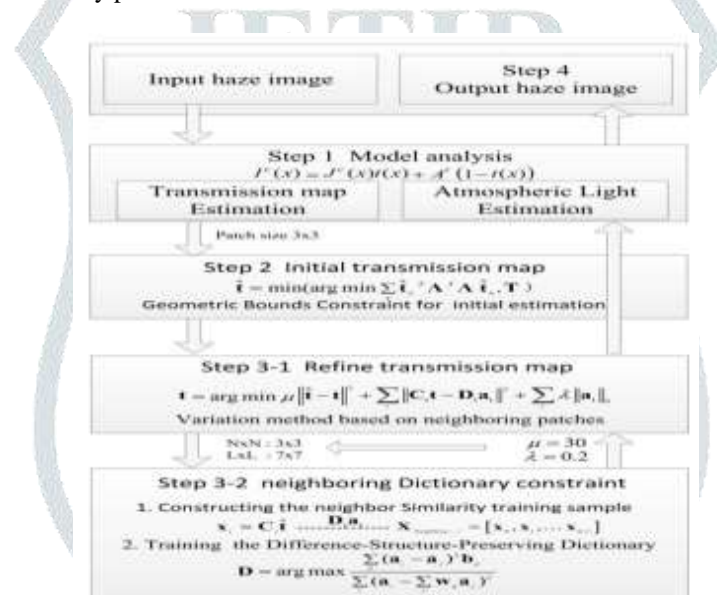


Fig4: DSPV flowchart

Technique to code each fix, which is known as the distinction structure - conservation dictionary. In view of the underlying dictionary utilizing the cross-intelligent technique and setting the opportunity, we can acquire dictionary D_i and codes $I a_i$. It ought to be noticed that this approach takes in the dictionary on the arrangement of covering patches with the goal that scanty image models can deal with such circumstances by abusing the redundancy between covering patches. At last, under the environmental light proposed by He^[12] an optimal transmission can be communicated as, is utilized for dehazing the image. In rundown, the proposed strategy keeps up the nearby consistency as well as mirrors the distinction of every pixel.

III. OBSERVABLE ASSESSMENT ON REAL IMAGES:

Evaluating reestablished images is an extremely troublesome errand since certifiable, without haze reference images have not been approved for measurement of reestablished images. To show the adequacy of our strategy, some genuine images of outside scenes and manufactured dim images are tried. Specifically, these manufactured images are taken from two Foggy Road Image Databases, which incorporate 84 uniform-haze images. Correlation for Different Haze Removal Algorithms. The technique is contrasted and that of Tan^[17] and DCP. As appeared by the outcomes, radiance antiques still exist in Tan's strategy, for example, in the zone between the tree trunks, which is been appeared in the red rectangular box^[19]. Then again, our technique can evacuate radiance relics viably and hold more points of interest in the tree trunks because of comparability in the neighborhood window for assessing the transmission delineate.

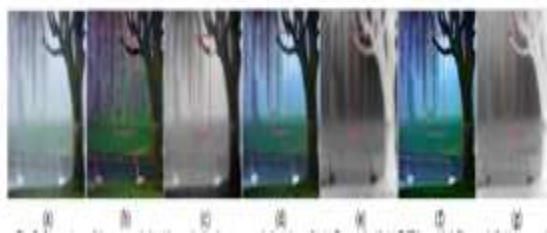


Fig5: Comparison of the proposed algorithm and other haze removal algorithms. (b) (c) Tan result, (d) (e) DCP by guided filter, and (f) (g) proposed method.



Fig6: Experimental result comparison.(a) Original image, (b) MSRCR result, (c) CLAHE result, (d) Our method.



Fig7: Haze removal results for pumpkin image. (a) Input image (b) result by[11] (c) result by[9] (d) result by [15] (e) result by [17] (f) result by [6] (g) result by [12] (h) result by the proposed algorithm.

Fig 7 shows the correlations with Nishino^[15], Fattal^[11], Fattal^[9]. Their techniques accomplish practically identical outcomes in sans haze images. For example, considers shading ellipsoids that can be fixing to depth signals inside an image. Nishino uses FMRF fields to appraise the albedo scene. DCP hypothesis and assessments haze thickness. Be that as it may, our transmission delineate more neighborhood subtle elements, so it genuinely mirrors the basic scene content by picking the nearby similitude. As appeared in Fig 8, the outcomes exhibit that our dehazing strategy has beaten alternate strategies as far as visual differentiation. This achievement originates from the exact estimation of our transmission outline. Interestingly, a lot of algorithms rely upon global priors or certain appropriations, which may create thick haze districts that will make them untrustworthy.



Fig.8. Comparison of the mainly dehazing methods. Besides the initial hazy images

As found in Fig 9. our administrator can yield similar and far better outcomes against the conventional dehazing systems. Tan's strategy^[17] creates numerous soaked pixels in Fig 9(c). since it just amplifies the differentiation. The technique for Tarel^[21] is computationally less confused, yet it changes shading tones and displays radiance antiquities, as appeared in Fig 9(f). The strategy for He^[12] just considers the darkest pixel esteem for dehazing, and it in this manner expels the shadow of the cloud as in Fig 9(d). Despite the fact that Nishino's strategy^[15] can improve the perceivability successfully, it expands the clamor, since it for the most part depends on MRF definition as opposed to fitting the haze show. The principle novel commitment of Kopf^[6] comprises of utilizing an unpleasant 3D delineate of the scene that enhances the nature of the scene^[20].



Fig.9. Results on stereo images where the ground truth solutions are known.(a) The hazy images (b) Tarel results (2009) (c) Tarel results (2010) (d) He results. (e) Our results (f) Ground truth

The technique for Fattal [12] yields more natural outcomes, however it can't adequately evacuate haze in a few districts, for instance. This exhibits the accomplishment as far as depth exactness and the adequacy of compelling both the smoothness and build safeguarding. In this way, the proposed algorithm can stifle a large portion of the antiques that happen in the conventional dehazing algorithms.

Table1: Qualitative Comparison of existing and proposed work is describes in the table

Image	metric	Existing Methods							Proposed	
		Fattal 08	Tan	He	Kopf	Tarel	Nishno	Fattal 14	Existing	Our
Building	<i>e</i>	-0.06	-0.14	0.06	0.05	0.07	-0.01	0.04	0.04	0.042
	Σ	0.09	0.02	0.00	0.00	0.00	0.46	0.00	0.01	0.01
	<i>r</i>	1.32	2.34	1.42	1.42	1.88	1.81	1.86	1.73	1.56
Landscape	<i>e</i>	0.04	0.08	0.08	0.09	0.02	0.11	0.03	0.05	0.04
	Σ	0.02	0.01	0.01	0.00	0.00	0.71	0.31	0.15	0.13
	<i>r</i>	1.23	2.28	1.33	1.62	2.09	1.79	1.83	1.82	1.81
Person	<i>e</i>	0.05	-0.03	0.03	0.05	0.04	0.12	0.10	0.11	0.09
	Σ	0.03	0.02	0.01	0.00	0.01	0.41	0.25	0.27	0.22
	<i>r</i>	1.15	2.32	1.52	1.52	2.22	2.19	1.93	2.04	1.86

This element is accomplished additionally by the techniques for Fattal [9], He [12] and Kopf [6]. The strategies of Tan [17] and Tarel [21] increment the nearby difference too emphatically, and therefore, these methodologies have higher estimations of pointer *r*, which shows the nearness of deceptive edges and antiques. To quantitatively evaluate and rate the algorithms, we utilized another appraisal strategy as a correlation record that depends on the mean-square blunder (MSE) and the basic closeness (SSIM) of the outcomes. As can be seen, the consequences of Tarel's technique deliver the most noteworthy MSEs by and large, which are for the most part because of the vast number of lingering fogs in the dehazed images. The scores of the aftereffects of He's [12] technique are better and are the second littlest out of all the methodologies. Our strategy accomplishes the most reduced MSEs in all cases. A high SSIM speaks to high comparability between the dehazed image and the ground-truth image, while a low SSIM passes on the contrary importance. The greater part of Tarel's outcomes are lower than the others, showing that much auxiliary data in the images has been lost. When all is said in done, the SSIMs of He [12] are substantially higher in these images, yet now and then the outcomes are not exceptionally steady and are infrequently even lower than Tarel's. Our outcomes accomplish the most astounding SSIMs because of spotlight on the auxiliary consistency all through the dynamic contrast structure-protection process.

IV. EXPERIMENTAL RESULTS



Fig 10:Original test image corrupted by haze and fog



Fig 9:Extracted Dark Channel From the Test Image



Fig 10: Estimated transmission map From the Test Image.



Fig 11: Filtered transmission map of the Test Image.



Fig 12: Refined transmission map of the Test Image.



Fig 13: Estimated radiance map of the Test Image.



Fig 14: Final haze and fog removed output.

V. CONCLUSION

This paper proposed a dehazing algorithm in view of the distinction structure-preservation prior, which can evaluate the optimal transmission delineate reestablish the real scene. To acquire the unpleasant transmission outline, utilize two fundamental properties in the haze model to determine the optimal parameter at a similar depth. Subsequently that an image fix can be approximated by a meager direct blend of components from a neighbor premise set to get a more exact transmission outline can better protect the structures of images. Test comes about were additionally used to check that the technique adequately accomplishes exact and genuine portrayal. Later on, this technique will be considered in global air-light to enhance operational productivity and focus on the issue of shading blunder, and further applications in video dehazing will be investigated.

REFERENCES

- [1] NAYAR, S. K., AND NARASIMHAN, S. G. 1999. Vision in bad weather. Proceedings of IEEE International Conference on Computer Vision (I CCV) '99, 820–827..
- [2] E. J. McCartney. —Scattering by Molecules and Particles,| in Optics of the Atmosphere, New York, John Wiley and Sons, 1976.
- [3] S. G. Narasimhan and S. K. Nayar, —Contrast Restoration of Weather Degraded Images,| IEEE Trans. Pattern Anal. Mac. Intell, vol. 25, no. 6, pp. 713–724, June. 2003.
- [4] K. B. Gibson , D. T. Võ , T. Q. Nguyen , —An Investigation of Dehazing Effects on Image and Video Coding,| IEEE Trans. Image Process, vol. 21, no. 2, pp. 662–673, Feb. 2012.
- [5] Z. Chen, B. R. Abidi, D. L. Page, and M. A. Abidi, —Gray-level grouping (GLG): An automatic method for optimized image contrast enhancement—Part II: The variations,| IEEE Trans. Image Process. Vol. 15, no. 8, pp. 2303–2314, Aug. 2006.
- [6] J. Kopf, B. Neubert, B. Chen, et al, —Deep photo: Model-based photograph enhancement and viewing,| ACM Trans. on Graphics, vol. 27, no. 5, pp. 32-39, Dec. 2008.
- [7] L. Li, W. Feng and J. W. Zhang, —Contrast enhancement based single image dehazing via TV-L1 minimization,| in Proc. IEEE intconf on Multimedia &Expo, Cheng Du, China, 2014, pp. 435-440.
- [8] L. Caraffa and J. P. Tarel, —Markov Random Field Model for Single Image Defogging,| in Proc. Of IEEE Intelligent Vehicles Symposium, Gold Coast, Australia, 2013, pp.994-999.
- [9] R. Fattal, —Single image dehazing,| ACM Trans. Graph, Vol. 27, no. 3, pp. 1–9, Aug. 2008.
- [10] Y. K. Wang, —Single Image Defogging by Multi-scale Depth Fusion,| IEEE Trans. Image Process, vol. 23, no. 11, pp. 4826–4837, Nov. 2014.
- [11] R. Fattal, —Dehazing using Color line,| ACM Trans. Graph, Vol. 34, no. 1, pp. 256–269, Nov. 2014.
- [12] K. He, J. Sun, and X. Tang, —Single image haze removal using dark channel Prior,| IEEE Trans. Pattern Anal. Mach. Intell. Vol. 33, no. 12, pp. 2341–2353, Dec. 2011.
- [13].Tomasi, C., Manduchi, R.: Bilateral filtering for gray and color images. ICCV (1998) 2. Levin, A., Lischinski, D., Weiss, Y.: A closed form solution to natural image matting. CVPR (2006)

- [14] Y.Y. Schechner, S.G. Narasimhan, and S.K. Nayar, "Instant Dehazing of Images Using Polarization," Proc. IEEE Conf. Computer Vision and Pattern Recognition, 2001.
- [15] K. Nishino, —Bayesian Defogging, Int. J. Computer. Vis, vol. 98, pp. 263-278, Nov. 2012.
- [16] Qingsong Zhu, Jiaming Mai, and Ling Shao, —A Fast Single Image Haze Removal Algorithm Using Color Attenuation Prior, IEEE Trans. Image Processing, vol.24, no. 11, pp. 3522–3533, Nov. 2015.
- [17] R. Tan, —Visibility in bad weather from a single image, in Proc. of IEEE Conf on Computer Vis and Pattern Recognition, Anchorage, Alaska, USA, 2008, pp. 1–8.
- [18] Y.Y. Schechner, S.G. Narasimhan, and S.K. Nayar, "Polarization Based Vision through Haze," Applied Optics, special issue: light and color in the open air, vol. 42, no. 3, Jan. 2003.
- [19] S. Shafer, "Using Color to Separate Reflection Components," Color Research and Applications, pp. 210-218, 1985.
- [20] C. Stauffer and W.E.L. Grimson, "Adaptive Background Mixture Models for Real-Time Tracking," Proc. IEEE Conf. Computer Vision and Pattern Recognition, 1999
- [21] J.-P. Tarel and N. Hauti`ere, —Fast visibility restoration from a single color or gray level image, in *Proceedings of IEEE International Conference on Computer Vision (ICCV'09)*, Kyoto, Japan, 2009, pp. 2201–2208

